J|A|C|S
COMMUNICATIONS

Published on Web 01/28/2006

4f−5f Heterotrimetallic Complexes Exhibiting Electrochemical and Magnetic Communication

Eric J. Schelter,[†] Jacqueline M. Veauthier,[†] Joe D. Thompson,[‡] Brian L. Scott,[†] Kevin D. John,[†] David E. Morris,*[,†] and Jaqueline L. Kiplinger*[,†]

Chemistry and Materials Science & Technology Divisions, Los Alamos National Laboratory, Los Alamos, New Mexico 87545

Received November 16, 2005; E-mail: demorris@lanl.gov; kiplinger@lanl.gov

The electronic structures of the early actinides have characteristics of both lanthanides (dominated by spin−orbit coupling) and transition metals (dominated by ligand field effects). A potential manifestation of this behavior for multimetallic complexes containing early actinides is metal−metal coupling mediated by bridging ligands. Coupling of electrons across properly tailored diamagnetic bridging ligands has been unambiguously observed for $[(MeC_5H_4)_3U]_2[\mu\text{-}1,4\text{-}N_2C_6H_4]$;[1] however, of the few polymetallic f-element species reported, most do not exhibit direct evidence for f-electron communication. Herein, we report the synthesis and characterization of unique heterotrimetallic molecular systems containing both lanthanide and actinide metal centers, which exhibit electronic properties consistent with metal−metal communication.

Reaction of $(C_5Me_5)_2An(CH_2C_6H_5)_2$ (An = U, Th) with 2 equiv of 4′-cyano-2,2′:6′,2″-terpyridine[2] in toluene affords the terpyridyl-functionalized ketimide complexes **1** and **2**.[3] These possess terpyridyl (tpy) groups suitable for the introduction of two additional metal ions and subsequently react with 2 equiv of $(C_5Me_5)_2Yb(OEt_2)$ to give the novel 4f−5f heterotrimetallic compounds **3** and **4** in greater than 65% yield (eq 1).[3]

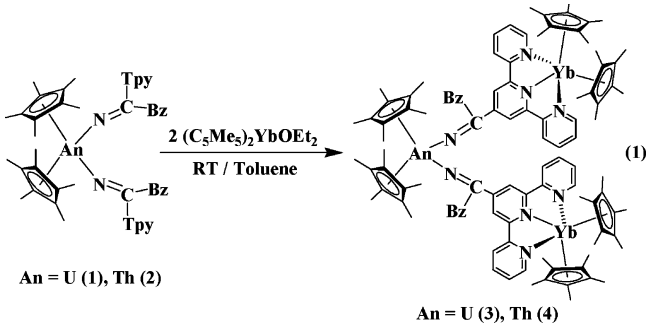

The molecular structure of **3** shown in Figure 1 is one of only three known structures of a complex containing both lanthanide and actinide ions.[4] Comparisons of the geometric parameters in **3** are rendered difficult by site occupancy disorder of the U(1) and Yb(2) centers. Nevertheless, the U−N distances and U−N−C angles in **3** fall within the ranges typically observed for U(IV) ketimide complexes;[5] the bond distances and angles at the Yb(1) site compare well with those reported for other ytterbocene terpyridine adducts.[6]

Recent work by our group has shown that both $(C_5Me_5)_2Yb(tpy)$ (**5**) and $(C_5Me_5)_2Yb(tpy\text{-}CN)$ (**6**) exist in temperature-dependent valence equilibria between $4f^{13}\text{-}\pi^{*1}$ Yb(III)tpy$^{\bullet-}$ and $4f^{14}\text{-}\pi^{*0}$ Yb(II)tpy states, with Yb(II) being the lowest energy configuration.[7] Therefore, **3** and **4** might experience this same equilibrium between valence isomers with the potential added complexities resulting from multiple ytterbocene centers, a 5f metal center bridging these lanthanide species, and, for **3**, the opportunity for additional redox states for this bridging U metal center. The room-temperature UV−visible-near-IR absorption spectral data[3] are consistent with the presence of paramagnetic $4f^{13}\text{−}\pi^{*1}$ Yb(III)tpy$^{\bullet-}$ moieties in both **3** and **4** as evidenced by intense, low-energy $\pi\text{−}\pi^*$ and $\pi^*\text{−}\pi^*$ transitions.

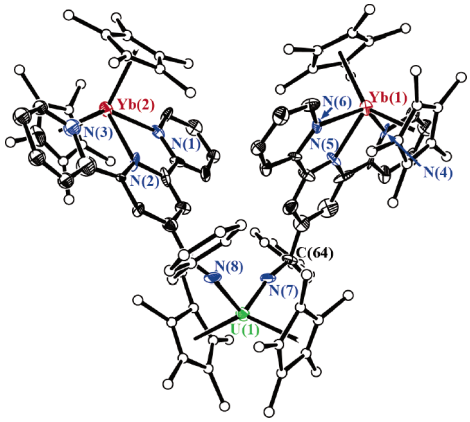

Figure 1. Molecular structure of **3** with thermal ellipsoids at the 30% probability level. Cyclopentadienyl and benzyl carbons shown as spheres of arbitrary radius for clarity. Selected bond distances (Å) and angles (deg): U(1)−N(7) 2.054(8), U(1)−N(8) 2.135(8); N(7)−C(64) 1.369(11), N(8)−C(21) 1.313(11); U(1)−N(7)−C(64) 168.7(7), U(1)−N(8)−C(21) 168.4(7); Yb(1)−N(4) 2.384(2), Yb(1)−N(5) 2.357(4), Yb(1)−N(6) 2.414(4), Yb(2)−N(1) 2.467(2), Yb(2)−N(2) 2.382(4), Yb(2)−N(3) 2.430(7).

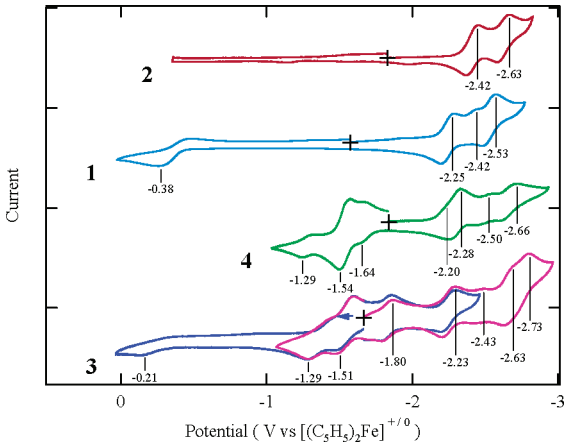

Figure 2. Cyclic voltammograms in 0.1 M $[(n\text{-}C_4H_9)_4N][B(C_6F_5)_4]$/THF at 200 mV/s.

Cyclic voltammetric data for **1**−**4** are shown in Figure 2.[3] The reduction waves for **2** are attributed to successive 1e$^-$ processes for each of the two tpy fragments. Similarly, the two prominent reduction waves for **1** (−2.25 and −2.53 V) are ascribed to the

[†] Chemistry Division.
[‡] Materials Science & Technology Division.

10.1021/ja057808+ CCC: $33.50

same processes. Although these tpy-based processes might be expected to be isoenergetic since the tpy fragments are separated by >12 Å, they are well resolved (210 and 282 mV, respectively). The resolution and the difference in the potential separation for these two waves in **1** vs **2** (71 mV) imply that the tpy−tpy interaction is through-bond in character with the difference attributable to a greater participation of the U vs Th valence orbitals in bonding to the ketimide bridges to facilitate the larger interaction between the peripheral tpy fragments. The additional U(V/IV) and U(IV/III) waves for **1** are seen at −0.38 V and −2.42 V, respectively. This assignment is consistent with all previous voltammetric data on U(IV) ketimides,[5,8] including the benchmark ∼2.1 V separation between these redox steps for a broad range of U(IV) metallocenes.

The increase in complexity of the voltammetric data for **3** and **4** precludes a complete, unambiguous assignment of all waves. However, by comparing these data to those for complexes **1**, **2**, **5**, and **6**, it is possible to derive some general conclusions. In **5** and **6**, the room-temperature voltammetry is dominated by a Yb(III) reduction wave and a tpy$^{\bullet-}$ oxidation wave deriving from the nominal $4f^{13}-\pi^{*1}$ Yb(III)tpy$^{\bullet-}$ electronic configuration of the major room-temperature species, the paramagnetic redox isomer.[7] Thus, for **3** and **4**, such an electronic configuration on the ytterbocene fragments would account for two reduction waves and two oxidation waves of comparable peak current. For **3**, one would also expect U-based waves for both oxidation and reduction. The wave at −0.21 V for **3** is the only candidate for the U-based oxidation. The most probable candidates for the U-based reduction wave are those at −2.63 and −2.73 V since this process should be shifted to more negative potentials than those in **1** as a consequence of the negative charges on the tpy ligands. However, this does not account for all observed waves. There are three additional waves for **4** and two for **3**. These are likely attributable to processes for the redox isomers containing diamagnetic $4f^{14}-\pi^{*0}$ Yb(tpy) centers that are apparently present in sufficient concentrations at room temperature to exhibit resolved voltammetric waves.

The temperature-dependent magnetic susceptibility of **1** and **4** are provided as Supporting Information. The χT vs T product of **1** decreases monotonically with decreasing temperature, as expected for an f^2-U(IV) ion.[9] The susceptibility of **4** closely follows the expected behavior from **6**,[7] consistent with a temperature-dependent electron transfer between the Yb ions and the tpy groups. The value of χT vs T at 350 K of 4.29 emu K mol^{-1} for **3** is less than the calculated value based on twice the reported χT product for complex **6** at this temperature ($2 \times 2.69 = 5.38$ emu K mol^{-1}), a difference that can be ascribed to the change in electron-withdrawing ability of the tpy moiety upon conversion of its substituent from nitrile to ketimide. Such a change in electronic structure and magnetic moment is consistent with the known electronic sensitivity of the ytterbocene−polypyridyl system.[7] The similarities in the response of **4** and **6** indicate no Th(IV)-mediated magnetic coupling is occurring between the reduced ligands at low temperatures within the paramagnetic fraction.

As shown in Figure 3, the χT product of **3** decreases gradually with decreasing temperature over most of the range until it reaches ∼25 K, where it abruptly decreases. The overall character of the susceptibility response of **3** indicates a nontrivial combination of the depopulation of crystal field levels of the U(IV) and Yb(III) ions and the thermally induced charge transfer exhibited by the Yb−tpy moiety. Due to the strong temperature dependences of these components, the susceptibility of **3** does not unambiguously demonstrate the existence of magnetic coupling.

Application of a modified version of the subtraction method of Kahn and Costes[10] to the magnetic data for **3** yielded the response

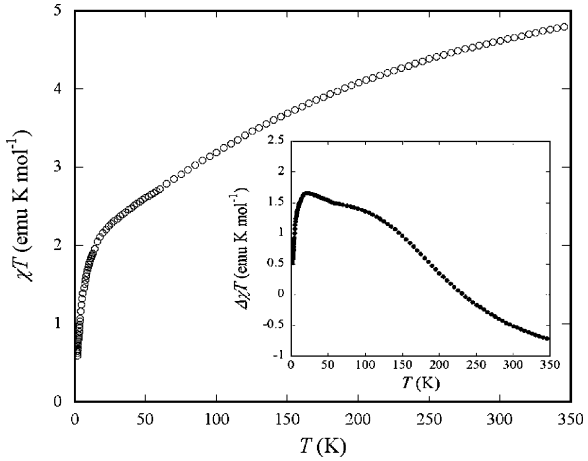

Figure 3. Magnetic susceptibility of **3** between 2 and 350 K and Δ (χT(**3**)−χT(**1**)−χT(**4**)) between 2 and 60 K (inset).

shown in the inset of Figure 3. In the absence of magnetic coupling $\Delta\chi T$ should be zero over the whole temperature range. The inset shows the $\Delta\chi T$ response achieves a maximum at 20 K then decreases precipitously below ∼15 K, which suggests the presence of magnetic coupling in **3**. Inspection of the $\Delta\chi T$ vs T data over the whole temperature range indicates the subtraction of the χT signal for **4** is overcorrecting for that observed in **3**, such that the exact nature of coupling cannot be ascertained in these experiments.[3] The sigmoidal shape between 350 and ∼60 K indicates differences in the electronic structures of the An−N═C(Bz)(tpy) moiety for Th vs U, which is in agreement with the voltammetric data for these systems. This yields a change in the valence equilibrium of the ligand, resulting in a difference in the temperature-dependent susceptibility of **3**. Nevertheless, at 230 K, $\Delta\chi T$ becomes positive and continues to increase until reaching its maximum. The $\Delta\chi T$ response indicates that, despite the overcorrection, magnetic coupling between the U(IV) and Yb(III)tpy$^{\bullet-}$ groups is present at low temperatures in this complex.

Acknowledgment. For financial support, we acknowledge the LANL G. T. Seaborg Institute (Postdoctoral Fellowships to E.J.S. and J.M.V.), the LANL LDRD Program, and the Division of Chemical Sciences, Office of Basic Energy Sciences.

Supporting Information Available: Full experimental and spectroscopic details for all compounds, crystallographic data for **1** and **3** (CIF), and magnetic susceptibility data for **1**, **3**, and **4**. This material is available free of charge via the Internet at http://pubs.acs.org.

References

(1) Rosen, R. K.; Andersen, R. A.; Edelstein, N. M. *J. Am. Chem. Soc.* **1990**, *112*, 4588−4590.
(2) Veauthier, J. M.; Carlson, C. N.; Collis, G. E.; Kiplinger, J. L.; John, K. D. *Synthesis* **2005**, *16*, 2683−2686.
(3) See Supporting Information for additional details.
(4) Leverd, P. C.; Rinaldo, D.; Nierlich, M. *J. Chem. Soc., Dalton Trans.* **2002**, 829−831.
(5) Jantunen, K. C.; Burns, C. J.; Castro-Rodriguez, I.; Da Re, R. E.; Golden, J. T.; Morris, D. E.; Scott, B. L.; Taw, F. L.; Kiplinger, J. L. *Organometallics* **2004**, *23*, 4682−4692 and references therein.
(6) Kuehl, C. J.; Da Re, R. E.; Scott, B. L.; Morris, D. E.; John, K. D. *Chem. Commun.* **2003**, 2336−2337.
(7) Veauthier, J. M.; Schelter, E. J.; Kuehl, C. J.; Clark, A. E.; Scott, B. L.; Morris, D. E.; Martin, R. L.; Thompson, J. D.; Kiplinger, J. L.; John, K. D. *Inorg. Chem.* **2005**, *44*, 5911−5920.
(8) Morris, D. E.; Da Re, R. E.; Jantunen, K. C.; Castro-Rodriguez, I.; Kiplinger, J. L. *Organometallics* **2004**, *23*, 5142−5153.
(9) Boudreaux, E. A.; Mulay, L. N. *Theory and Applications of Molecular Paramagnetism*; Wiley: New York, 1976.
(10) (a) Costes, J.-P.; Dahan, F.; Dupuis, A.; Laurent, J.-P. *Chem.—Eur. J.* **1998**, *4*, 1616−1620. (b) Salmon, L.; Thuery, P.; Riviere, E.; Girerd, J. J.; Ephritikhine, M. *Dalton Trans.* **2003**, 2872−2880. (c) Sutter, J. P.; Kahn, M. L. *Magnetism: Molecules to Materials V* **2005**, 161−187.

JA057808+